ARTICLE TYPE

Theoretical evidence for the direct ^{3}MLCT-HS deactivation in the light-induced spin crossover of Fe(II)-polypyridyl complexes†

Carmen Sousa,[a] Miquel Llunell,[a] Alex Domingo,[b] and Coen de Graaf[*,b,c]

Spin-orbit couplings have been calculated in twenty snapshots of a molecular dynamics trajectory of $[Fe(bpy)_3]^{2+}$ to address the importance of geometrical distortions and second-order spin-orbit coupling on the intersystem crossing rate constants in the light-induced spin crossover process. It was found that the effective spin-orbit coupling between the ^{3}MLCT and $^5T_2$ state is much larger than the direct coupling in the symmetric structure, which opens the possibility of a direct ^{3}MLCT-$^5T_2$ deactivation without the intervention of triplet metal-centered states. Based on the calculated deactivation times, we conclude that both the direct pathway and the one involving intermediate triplet states are active in the ultrafast population of the metastable HS state, bringing in agreement two experimental observations that advocate for either deactivation mechanism. This resolves a long-standing dispute about the deactivation mechanism of Fe(II)-polypyridyl complexes in particular, and about light-induced magnetism in transition metal complexes in general.

1 Introduction

Light-induced spin crossover (SCO) is a very useful phenomenon when it comes to the development of switchable devices. The existence of two different, easily accessible electronic states at constant temperature makes the molecular-based systems that present such behavior well-suited building blocks for real-world applications.[1–3] Fe(II) complexes with six-fold coordination through nitrogen are prototypical SCO systems, whose singlet to quintet spin conversion is typically accompanied by significant structural changes and has been observed both in solids and solutions with high quantum efficiency. The iron(II) tris(bipyridine) complex $[Fe(bpy)_3]^{2+}$ in aqueous solution is a paradigmatic system for the investigation of SCO under the influence of light and has been studied extensively both experimentally and by means of computational approaches. The study of the deactivation mechanisms of this system by several ultrafast optical and X-ray spectroscopic techniques has generated profuse discussions and led to a vast literature,[4–14] yet there are still several points that need to be clarified for a full understanding of the photocycle.

Irradiation with visible light excites the system to a singlet metal-to-ligand charge-transfer (^{1}MLCT) state followed by a decay into the metal-centered (MC) $^5T_2$ high-spin (HS) state on a femtosecond time scale with almost unity quantum yield. It is generally accepted that the first step in the deactivation process involves a singlet to triplet conversion within the MLCT manifold, which takes place in about 30 fs. Subsequently, the system evolves into an excited vibrational level of the HS quintet state in less than 150 fs. Vibrational cooling in the HS state has been estimated to take a few picoseconds while the decay to the low-spin (LS) ground state happens within 650 ps.[15]

Whereas the character of the first intersystem crossing (from singlet to triplet spin) is clearly established, there is more discussion about the triplet-quintet spin conversion. According to some studies, the spin crossover follows a two-step intersystem crossing deactivation path ^{1}MLCT $\rightarrow$ ^{3}MLCT $\rightarrow$ ^{5}T avoiding intermediate singlet and triplet MC states.[15] Other authors suggested a mechanism in which mixtures of excited states lying between the ^{1}MLCT and $^5T_2$ states are involved.[11]

From the outcomes of *ab initio* multiconfigurational electronic structure calculations, we have proposed an alternative mechanism involving intermediate MC triplet states between the ^{3}MLCT and the final HS quintet state.[12] Since the direct spin-orbit coupling between ^{3}MLCT and $^5T_2$ is extremely small, it was concluded that the ^{3}MLCT $\rightarrow$ ^{5}T intersystem crossing is not very ef-

[a] *Departament de Ciència de Materials i Química Física and Institut de Química Teòrica i Computacional, Universitat de Barcelona, C/ Martí i Franquès 1, 08028 Barcelona, Catalunya, Spain*

[b] *Departament de Química Física i Inorgànica, Universitat Rovira i Virgili, Campus Sescelades, 43007 Tarragona, Catalunya, Spain.*

[c] *ICREA, Pg. Lluís Companys 23, 08010, Barcelona, Catalunya, Spain; E-mail: coen.degraaf@urv.cat*

ficient. Instead a much faster pathway was established through two triplet states centered on the metal: $^{(1,3)}$MLCT $\rightarrow$ ^{3}T $\rightarrow$ ^{5}T. Similar conclusions were derived from X-ray fluorescence spectroscopy measurements with femtosecond resolution.[13] However, these results are challenged by recent transient absorption experiments with time resolutions of 40-60 fs.[14] This study points to a direct conversion from the MLCT manifold to the ^{5}T$_2$ in less than 50 fs, meaning that the process occurs on a much shorter time scale than previously reported. The identical times measured for the MLCT decay and the HS state population implies that no intermediate states are involved. Altogether, the complexity of the problem is evident, as different interpretations can be derived from the experimental and theoretical studies performed.

So far, the theoretical description of the intersystem crossing only considered the direct (or first-order) spin-orbit coupling between the participating states. However, for a complete treatment one should also introduce the indirect coupling between these states mediated by other (excited) states. Furthermore, the structural disorder due to thermal agitation breaks the symmetry of the average equilibrium structure, which could introduce variations in the calculated spin-orbit coupling.

Here, we show that taking into account structural disorder and second-order spin-orbit coupling changes the existing theoretical picture profoundly. Certain geometrical distortions activate the spin-orbit coupling between the ^{3}MLCT and ^{5}T$_2$ states to such an extent that the intersystem crossing becomes at least as fast as the one involving the MC triplet states. Hence, we provide theoretical evidence for the efficiency of the direct ^{3}MLCT $\rightarrow$ ^{5}T deactivation pathway, as seen recently by transient absorption spectroscopy. Since the calculated intersystem crossing rate constant is of similar order of magnitude as for the previously proposed pathway involving the MC triplets, we advocate for a deactivation mechanism via two competitive pathways. A scenario that may very well be at the origin of the different interpretations of the deactivation in the two recently published experimental studies.[13,14]

2 Second-order spin-orbit coupling by effective hamiltonian theory

Before discussing the results obtained, we first shortly expose the procedure that we have developed to accurately calculate the second-order spin-orbit coupling using effective Hamiltonian theory[16–18]. Usually, this coupling is estimated through perturbation theory as the sum of the direct interaction between states Φ_i and Φ_j and the simultaneous interaction of these states with intermediate states Φ_α:

$$H_{ij}^{SO} = \langle \Phi_i | \hat{H}^{SO} | \Phi_j \rangle + \sum_{\alpha \neq i, j} \frac{\langle \Phi_i | \hat{H}^{SO} | \Phi_\alpha \rangle \langle \Phi_\alpha | \hat{H}^{SO} | \Phi_j \rangle}{E_\alpha - E_j} \quad (1)$$

but this approach leads unavoidably to unreliable results when states i and j do not correspond to the lowest states of the system under study. For instance, in the calculation of the spin-orbit coupling between ^{3}MLCT and ^{5}T$_2$ –two electronically excited states in the Franck-Condon region– there are intermediate states α with very similar, or even lower, energy. This will lead to very small or negative denominators in the perturbative expression,

and hence, unreliable estimates of the coupling.

Instead, we use a variational approach based on effective Hamiltonian theory, which avoids the use of energy denominators, and hence, is generally applicable contrary to the perturbative approach. The procedure maps a large spin-orbit matrix S onto a smaller model space S_0. The resulting effective spin-orbit matrix elements $H_{ij}^{SO,eff}$ give a direct measure of the effective coupling between the states i and j. In the first place, the spin-orbit matrix elements $\langle \Phi_i | \hat{H}^{SO} | \Phi_j \rangle$ are calculated among all the basis functions $\Phi = \{\Phi_a, \Phi_b, \Phi_c, \ldots, \Phi_\alpha, \Phi_\beta, \ldots\}$ that span the N-dimensional Hilbert space S. Then the N eigenfunctions Ψ_p and energy eigenvalues E_p are determined by diagonalization of the matrix, where

$$\Psi_p = c_{p,a}\Phi_a + c_{p,b}\Phi_b + c_{p,c}\Phi_c + \ldots + c_{p,\alpha}\Phi_\alpha + c_{p,\beta}\Phi_\beta + \ldots$$

$$\Psi_q = c_{q,a}\Phi_a + c_{q,b}\Phi_b + c_{q,c}\Phi_c + \ldots + c_{q,\alpha}\Phi_\alpha + c_{q,\beta}\Phi_\beta + \ldots \quad (2)$$

etc.

Notice that the eigenfunctions and energy eigenvalues of the matrix are the result of the full interactions between all the states that span the space S, and hence, Ψ_p and E_p have incorporated not only the effect of the direct spin-orbit coupling, but also second-order (and higher orders) spin-orbit coupling.

The second step of the procedure consists in defining a smaller subspace of S, the so-called model space S_0. This model space is spanned by m ($m < N$) basis functions of the full space S, $\Phi_0 = \{\Phi_a, \Phi_b, \ldots, \Phi_m\}$, containing exactly those functions for which the second-order spin-orbit has to be calculated. The remaining $N - m$ basis functions $\{\Phi_\alpha, \Phi_\beta, \ldots \Phi_\omega\}$ are usually referred to as the external functions.

The next step in the procedure is to calculate the projections of all Ψ_p onto S_0

$$\widetilde{\Psi}_p = \sum_{k \in S_0} c_{p,k}\Phi_k \quad (3)$$

and select the m projections with the largest norm $\sum_{k \in S_0} |c_{p,k}|^2$. These m projections are neither mutually orthogonal nor normalized, and hence, before constructing the effective Hamiltonian an orthonormalization step is to be taken. Among the different orthogonalization schemes, we opt for the symmetric orthogonalization of des Cloizeaux[19] which involves the overlap matrix $S^{-\frac{1}{2}}$.

$$\widetilde{\Psi}_k^\perp = S^{-\frac{1}{2}}\widetilde{\Psi}_k \quad (4)$$

Now, the effective Hamiltonian can be constructed using the orthonormalized projections $\widetilde{\Psi}_k^\perp$ and the corresponding energy eigenvalues E_k by Bloch's formula[20]

$$H_{ij}^{SO,eff} = \langle \Phi_i | \hat{H}^{SO,eff} | \Phi_j \rangle = \langle \Phi_i | \left\{ \sum_{k \in S_0} |\widetilde{\Psi}_k^\perp\rangle E_k \langle\widetilde{\Psi}_k^\perp| \right\} | \Phi_j \rangle \quad (5)$$

By construction, the energy eigenvalues of this effective Hamiltonian are identical to E_k and the eigenfunctions of the matrix are the same as the orthonormalized projections of the eigenfunctions of the full space S. This means that the matrix elements $H_{ij}^{SO,eff}$ have incorporated not only the effect of the direct spin-orbit cou-

pling but also the effects of second-order and higher order spin-orbit couplings.

3 Results

The model space S_0 contains all the M_S-components of the spin states that are possibly involved in the deactivation. Apart from the initial LS (^{1}A) state and the final HS (^{5}T$_2$) states, we also consider the ^{1}MLCT, ^{3}MLCT and intermediate triplet ligand-field states (^{3}T$_1$ and ^{3}T$_2$), giving a model space spanned by 38 basis functions. The total space S has a dimension of 150×150 and is spanned by the M_S components of the lowest 12 singlets, 26 triplets and 12 quintets with ligand-field or MLCT character.

The structural disorder is taken into account by performing the calculations of the spin-orbit coupling on a collection of 20 snapshots along a molecular dynamics trajectory of [Fe(bpy)$_3$]$^{2+}$ in water at 300 K.[21] This collection gives a representative sample of the structural deformations of the LS state of the complex. Given the extremely fast deactivation of the excited state, it is reasonable to assume that the whole process takes place in the Franck-Condon region (that is, around the LS equilibrium geometry) and that the expansion of the Fe coordination sphere takes place during the vibrational cooling of the HS state. A detailed description of the computational details can be found in section 5

3.1 Effective spin-orbit coupling

Table 1 summarizes the direct and second-order spin-orbit coupling between the ^{3}MLCT and ^{5}T$_2$ state in the twenty conformations. Considering that there are 45 spin-orbit matrix elements (3 M_S-components of the ^{3}MLCT and 3×5 from the ^{5}T$_2$), we only list the average and the maximum values. Both quantities show the same general trend: a moderate increase of the spin-orbit coupling when the indirect interactions are taken into account through the effective Hamiltonian approach. The impact of the second-order coupling varies from close to negligible in some conformations (for instance, conformations 4, 6, 13 and 20) to more than doubling the direct interaction in others (conformations 7 and 15). However, the effect of the geometrical distortions on the spin-orbit coupling is even more remarkable. The average spin-orbit coupling ranges from 7 cm^{-1} for conformation 3 to 48 cm^{-1} calculated for conformation 14. The maximum effective spin-orbit coupling is over 100 cm^{-1} in six of the twenty conformations and reaches a maximum value of 182 cm^{-1} for conformation 6. Recalling that the average and the maximum spin-orbit couplings in the symmetric D_3 structure are 1.3 and 5.3 cm^{-1}, it is clear that structural distortions cannot be neglected in the analysis of the deactivation mechanism of the light-induced SCO of transition metal complexes.

3.2 ^{3}MLCT lifetime

The next step is to quantify to what extent the observed increase in the spin-orbit coupling between ^{3}MLCT and ^{5}T$_2$ leads to fast intersystem crossings between these states. For this purpose, we have applied Fermi's golden rule[22] to calculate the lifetime of the ^{3}MLCT state in the twenty conformations as reported in the fourth column of Table 1. Apart from the increased spin-orbit

Table 1 Average and maximum spin-orbit coupling between the ^{3}MLCT and ^{5}T$_2$ states and lifetime of the ^{3}MLCT state in the intersystem crossing for twenty snapshots along a molecular dynamics trajectory.

Conformation	Average SOC$^{(a)}$	Maximum SOC$^{(a)}$	Lifetime/fs
1	8 / 14	27 / 44	2063 / 872
2	19 / 21	47 / 64	337 / 305
3	7 / 7	24 / 30	2183 / 2889
4	31 / 33	133 / 132	117 / 112
5	12 / 14	49 / 56	627 / 608
6	45 / 46	182 / 182	56 / 56
7	11 / 28	35 / 92	1098 / 223
8	32 / 43	132 / 131	116 / 84
9	12 / 13	43 / 41	976 / 858
10	11 / 13	50 / 52	788 / 666
11	22 / 30	83 / 98	243 / 166
12	28 / 32	122 / 139	144 / 118
13	25 / 27	89 / 90	189 / 182
14	33 / 48	134 / 164	97 / 58
15	6 / 16	45 / 72	1679 / 562
16	8 / 13	38 / 56	1697 / 787
17	10 / 20	57 / 81	846 / 365
18	31 / 40	108 / 126	139 / 102
19	8 / 13	28 / 51	1930 / 1075
20	20 / 20	90 / 94	228 / 227
D_3 structure	1 / 2	5 / 8	/ > 10 ps

(a) direct / effective coupling, in cm^{-1}

contribution to the intersystem crossing rate, we have also taken into account that the relative energy of the ^{3}MLCT in the distorted structures is about 0.2 eV lower than in the symmetric structure as extensively discussed in Ref.[21]. We have used an energy difference between the ^{5}T$_2$ and ^{3}MLCT of 1.2 eV, corresponding to the separation of the maxima of the ^{3}MLCT and ^{5}T$_2$ absorption peaks in Fig. 6 of Ref.[21]. The combination of larger spin-orbit couplings and smaller energy differences drastically increases the intersystem crossing rate constants, and consequently, decreases the lifetime of the ^{3}MLCT along the direct deactivation pathway to the ^{5}T$_2$ state.

Fermi's golden rule can of course only give approximate lifetimes given the fact that it lacks non-adiabatic effects, but it has been proven to predict intersystem crossing rates of the right order of magnitude in quite a lot of different situations. Taking this as a guideline for deciding whether the estimate of the lifetime in the different conformation is compatible with a fast direct ^{3}MLCT-^{5}T$_2$ deactivation, it is obvious that the lifetimes in conformations 1, 3, 9, 16 and 19 are too long to warrant the mechanism proposed by Auböck and Chergui.[14] However, in other conformations the lifetime is much shorter, and assuming an uncertainty of a factor of 5, we conclude that the calculated lifetimes of the ^{3}MLCT $\rightarrow$ ^{5}T deactivation are in approximately 50% of the conformations small enough to be compatible with the 50 fs measured by Aubčk and Chergui. In the other conformations, the system may decay along the pathway that was previously suggested, namely the one that involves the MC triplet states. In a preceding study of the second-order spin-orbit coupling,[23] we have established that the spin-orbit coupling between the MC states is nearly unaffected by the indirect coupling and the geometrical distortions, while the coupling between the $^{(1,3)}$MLCT and the triplet MC states is indeed affected but to a much lesser extent than in the ^{3}MLCT-^{5}T$_2$ interaction. This means that the previously calculated deactivation time for the ^{1}MLCT $\rightarrow$ ^{3}MLCT $\rightarrow$ ^{3}MC $\rightarrow$ ^{5}T

pathway of $\sim$100 fs is still valid and that it can compete with the direct ^{1}MLCT $\rightarrow$ ^{3}MLCT $\rightarrow$ ^{5}T deactivation.

3.3 Possible relation between lifetimes and structural distortions

One last remaining issue is the question why the spin-orbit coupling is so strongly enhanced in some of the conformations, while it remains relatively small in others. The most straightforward hypothesis is to relate this variation with the degree of distortion away from the quasi-octahedral coordination sphere of the Fe(II) ion. To quantify the distortions, we have calculated the continuous shape measures (CSM) [24,25] of the 20 conformations, focusing on the octahedral-like FeN$_6$ core structure and the triangular position of the full ligands by considering the midpoints of the C-C bonds that connect the pyridine rings of the bipyridines. In the first place, we observe that the continuous symmetry measures are rather small, less than 1 on a scale that can reach values as large as 100, being 0 the value for the ideal centered octahedron and the C_3 triangle. Furthermore, there is no clear relation between the degree of distortions and the calculated spin-orbit coupling or lifetime of the ^{3}MLCT state. A full 61 atoms structure continuous shape measure has been also calculated. However, no shape path correlation has been found for the calculated spin-orbit parameters. Simpler analysis in which we have related one specific geometrical parameter (Fe-N average bond distance, bite angle of the ligands, twisting angle of the pyridine rings with respect to each other, etc.) with the size of the spin-orbit coupling all give similar pictures of very poor correlations. The supporting information contains tables relating the calculated SO-couplings and lifetimes with the symmetry measures and the different individual geometrical parameters.[†] Apparently, the relation between geometry and the magnitude of the spin-orbit coupling is a very subtle one, probably due to the small energy scale of the spin-orbit coupling. The variations that we observe are within a 1000 cm^{-1} energy range.

4 Conclusions

In conclusion, the second-order spin-orbit coupling combined with structural distortions provide a mechanism that activates the coupling between the ^{3}MLCT and ^{5}T$_2$ state, opening the direct deactivation pathway in addition to the one that involves intermediate metal-centered triplet states. This two-mode deactivation of the excited singlet state of the paradigmatic [Fe(bpy)$_3$]$^{2+}$ complex is most probably generally applicable for the whole family of Fe(II)-polypyridyl complexes. Furthermore, geometrical distortions and second-order spin-orbit coupling should also be taken into account in the theoretical description of light-induced spin crossover in complexes with other transition metals and ligands.

5 Computational Information

Second-order spin-orbit couplings were calculated with a homemade program to construct effective Hamiltonians using the *ab initio* wave functions and energies of the M_S components of the above mentioned electronic states as only input. These wave functions and energies were calculated with the

CASSCF/CASPT2/RASSI approach,[26] previously used in many other studies of systems where spin-orbit coupling plays a fundamental role and demonstrated to be a rather accurate method.[27–29] The 20 conformations of the [Fe(bpy)$_3$]$^{2+}$ complex are picked from the Car-Parrinello molecular dynamics simulation described in Ref.[21]. The complete active space used in the CASSCF calculations contains 13 orbitals and 10 electrons (see supporting information)[†] and the basis set has (6s,5p,4d,2f) functions on Fe, (4s,3p,1d) functions on N, (3s,2p) on C and (2s) on H. An imaginary level shift of 0.2 hartree is used to avoid intruder states in the CASPT2 calculations. We have used the standard IPEA zeroth-order Hamiltonian.

The lifetimes of the ^{3}MLCT state in the intersystem crossing with the ^{5}T$_2$ state are calculated using Fermi's golden rule transformed to the time-domain.[22] The expression for the intersystem crossing rate constant reads

$$k_{ISC} = |\langle \Phi_i | \hat{H}^{SO,eff} | \Phi_j \rangle|^2 \int_{-\infty}^{\infty} dt\, G(t) e^{it(\Delta E_{ij} + \frac{1}{2}Tr\Omega_i)}. \quad (6)$$

ΔE_{ij} is the CASPT2 energy difference between the ^{3}MLCT and ^{5}T$_2$, defined as the separation of the maxima of the peaks assigned to these states in the calculated absorption spectrum.[21] $\hat{H}^{SO,eff}$ is the effective Hamiltonian as defined in section 2 and $\langle \Phi_i | \hat{H}^{SO,eff} | \Phi_j \rangle$ the corresponding effective Hamiltonian matrix elements. The electronic coupling that enters the calculation of k_{ISC} is the sum of the squared matrix elements divided by the degeneracy of the initial state $(2S+1) \cdot (2L+1) = 3$. The explicit formula of the time dependent correlation function G(t) is rather lengthy and can be found in Ref.[22]. It contains the vibrational frequencies of the two states (Ω_i and Ω_j) and the Duschinsky matrix used to express the normal vibrational coordinates of the final state in those of the initial state. These quantities were calculated with density functional theory (PBE0/def2-TZVP) in our previous study of the complex reported in Ref.[12]

Conflict of interest

There are no conflicts to declare.

Notes and references

1 S. Hayami, S. M. Holmes and M. A. Halcrow, *J. Mater. Chem. C*, 2015, **3**, 7775–7778.

2 O. Sato, *Nature Chem.*, 2016, **8**, 644–656.

3 M. D. Manrique-Juárez, S. Rat, L. Salmon, G. Molnár, C. M. Quintero, L. Nicu, H. J. Shepherd and A. Bousseksou, *Coord. Chem. Rev.*, 2016, **308**, 395–408.

4 C. Bressler, C. Milne, V.-T. Pham, A. ElNahhas, R. M. van der Veen, W. Gawelda, S. Johnson, P. Beaud, D. Grolimund, M. Kaiser, C. N. Borca, G. Ingold, R. Abela and M. Chergui, *Science*, 2009, **323**, 489–492.

5   G. Vankó, P. Glatzel, V.-T. Pham, R. Abela, D. Grolimund, C. N. Borca, S. L. Johnson, C. J. Milne and C. Bressler, *Angew. Chem. Int. Ed.*, 2010, **49**, 5910–5912.

6   C. Bressler and M. Chergui, *Annu. Rev. Phys. Chem.*, 2010, **61**, 263–282.

7   R. Field, L. C. Liu, W. Gawelda, C. Lu and R. J. D. Miller, *Chem. Eur. J.*, 2016, **22**, 5118–5122.

8   B. E. Van Kuiken, H. Cho, K. Hong, M. Khalil, R. W. Schoenlein, T. K. Kim and N. Huse, *J. Phys. Chem. Lett.*, 2016, 465–470.

9   C. Consani, M. Premont-Schwarz, A. ElNahhas, C. Bressler, F. van Mourik, A. Cannizzo and M. Chergui, *Angew. Chem. Int. Ed.*, 2009, **48**, 7184–7187.

10 J. K. McCusker, K. N. Walda, R. C. Dunn, J. D. Simon, D. Magde and D. N. Hendrickson, *J. Am. Chem. Soc.*, 1992, **114**, 6919–6920.

11 C. Brady, J. J. McGarvey, J. K. McCusker, H. Toftlund and D. N. Hendrickson, *Spin crossover in Transition Metal Compounds III*, Springer-Verlag, 2004, vol. 235, pp. 1–22.

12 C. Sousa, C. de Graaf, A. Rudavskyi, R. Broer, J. Tatchen, M. Etinski and C. M. Marian, *Chem. Eur. J.*, 2013, **19**, 17541–17551.

13 W. Zhang, R. Alonso-Mori, U. Bergmann, C. Bressler, M. Chollet, A. Galler, W. Gawelda, R. G. Hadt, R. W. Hartsock, T. Kroll, K. S. Kjær, K. Kubiček, H. T. Lemke, H. W. Liang, D. A. Meyer, M. M. Nielsen, C. Purser, J. S. Robinson, E. I. Solomon, Z. Sun, D. Sokarasa, T. B. van Driel, G. Vankó, T.-C. Weng, D. Zhu and K. J. Gaffney, *Nature*, 2014, **509**, 345–348.

14 G. Auböck and M. Chergui, *Nature Chem.*, 2015, **7**, 629–633.

15 A. Cannizzo, C. J. Milne, C. Consani, W. Gawelda, C. Bressler, F. van Mourik and M. Chergui, *Coord. Chem. Rev.*, 2010, **254**, 2677–2686.

16 J.-P. Malrieu, P. Durand and J.-P. Daudey, *J. Phys. A*, 1985, **18**, 809–826.

17 J.-P. Malrieu, R. Caballol, C. J. Calzado, C. de Graaf and N. Guihéry, *Chem. Rev.*, 2014, **114**, 429–492.

18 C. de Graaf and R. Broer, *Magnetic Interactions in Molecules and Solids*, Springer, Heidelberg, 2015.

19 J. des Cloizeaux, *Nucl. Phys.*, 1960, **20**, 321–346.

20 C. Bloch, *Nucl. Phys.*, 1958, **6**, 329–347.

21 A. Domingo, C. Sousa and C. de Graaf, *Dalton Trans.*, 2014, **43**, 17838–17846.

22 M. Etinski, J. Tatchen and C. M. Marian, *J. Chem. Phys.*, 2011, **134**, 154105.

23 C. Sousa, A. Domingo and C. de Graaf, *Chem. Eur. J.*, 2017, in press.

24 H. Zabrodsky, S. Peleg and D. Avnir, *J. Am Chem. Soc.*, 1992, **114**, 7843–7851.

25 D. Casanova, J. Cirera, M. Llunell, P. Alemany, D. Avnir and S. Alvarez, *J. Am. Chem. Soc.*, 2004, **126**, 1755–1763.

26 P.-Å. Malmqvist, B. O. Roos and B. Schimmelpfennig, *Chem. Phys. Lett.*, 2002, **357**, 230–240.

27 P.-H. Lin, T. J. Burchell, L. Ungur, L. Chibotaru, W. Wernsdorfer and M. Murugesu, *Angew. Chem. Int. Ed.*, 2009, **48**, 9489–9492.

28 R. Maurice, R. Bastardis, C. de Graaf, N. Suaud, T. Mallah and N. Guihéry, *J. Chem. Theory Comput.*, 2009, **5**, 2977–2984.

29 L. Gagliardi, M. C. Heaven, J. W. Krogh and B. O. Roos, *J. Am. Chem. Soc.*, 2005, **127**, 86–91.
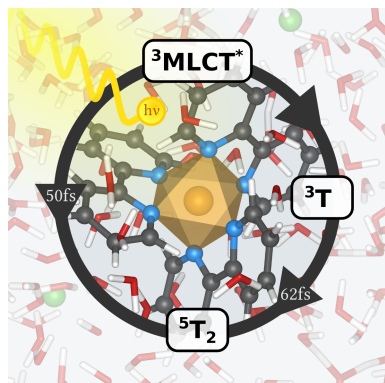
Graphical Table of Contents: Second-order spin-orbit coupling and structural distortions activate the ^{3}MLCT-^{5}T$_2$ deactivation in Fe(II)-polypyridyl complexes